American Journal of Modern Physics
2022; 11(1): 7-12
http://www.sciencepublishinggroup.com/j/ajmp
doi: 10.11648/j.ajmp.20221101.12
ISSN: 2326-8867 (Print); ISSN: 2326-8891 (Online)

Optical Interactions in Subwavelength Metallic Materials Array

Young-Chul Kim

Department of Optometry, Eulji University, Seongnam-si, Gyeonggi-do, Korea

Email address:
yckim@eulji.ac.kr

To cite this article:
Young-Chul Kim. Optical Interactions in Subwavelength Metallic Materials Array. *American Journal of Modern Physics*. Vol. 11, No. 1, 2022, pp. 7-12. doi: 10.11648/j.ajmp.20221101.12

Received: January 14, 2022; **Accepted:** February 17, 2022; **Published:** February 25, 2022

Abstract: When light is incident on the interface of different media, refraction and reflection occur. Also, while light propagates through a medium, scattering by particles constituting the medium is a well-known basic property. Recently, the non-classical phenomenon is expected to be the core of many technologies such as resonantly transfer energy, nanosized quantum optical energy amplifiers, and nano-sensing technique. This technique uses a surface plasmon induced by the reconfiguration of the distribution of electrons in a metallic material by stimulation of an external field. This is because, in the nanoscale structure of the medium, the light intensity distribution in the medium is changed by the interaction of the fields in the medium including the surface plasmon. In this study, the light transmission characteristics of the metal material array medium with a size smaller than the skin-depth were investigated by 3D simulation of the FDTD method. The light intensity distribution and light transmittance of the light passing through the medium of the metal (Au) cylinder and sphere array structure were analyzed. The synergistic effect of light transmittance appeared as the light spread was reduced due to the interaction between metal materials. In addition, when light is incident on the interface in an oblique direction, the beam peak is split into several parts.

Keywords: Skin-depth, Subwavelength Metal Array, Surface Plasmon, 3D Simulation

1. Introduction

Light control technology is the key to the possibility of using light. In terms of nano-optics, understanding the interaction of light with nano-sized materials is the basis for light control. When light reaches a material, it is scattered, and in a medium composed of a combination of materials, the distribution of light in space is changed by the overlap of each scattered light. At the metal-dielectric interface, the field distribution changes in space according to the relocation of free electrons on the metal surface by the external field at the interface, resulting in surface plasmon. The field by the surface plasmon affects the field distribution in the adjacent space or on the nearby metal surface. Due to this interaction, the beaming effect of the propagating light occurs and transmittance increases. [1, 2, 3, 4, 5, 6, 7, 8, 9] In addition, in a metal structure with periodicity, focusing and negative refraction occur in the light propagation process due to multiple interactions between them. [10, 11, 12]

In this study, the optical properties generated in a medium composed of a sub-skin-depth metal array were investigated through 3D simulation. In a metal plate lined up in the propagation direction, light interacts between adjacent plates in the transverse direction. As a result, the direction of the beam changes in the transverse direction, and the negative refraction phenomenon appears clearly.

In a periodic metal cylinder or metal sphere arranged perpendicular to the direction of light, the lateral interaction is relatively weak compared to that of the metal plate. However, multiple interactions in the longitudinal or diagonal directions occur simultaneously. As a result, the negative refraction caused by the lateral action is weakened. On the other hand, phenomena due to multiple interactions in the longitudinal or oblique direction may occur. [13, 14, 15] Therefore, in this study, the characteristics of transmitted light by metal cylinder array and sphere array were analyzed. The material of the metal cylinder and sphere analyzed in this study is Au. The

skin depth of Au is ∼25 nm and the relative permittivity is $\epsilon = -16.5 + 1.06i$. And for metal properties, Lorentz-Drude model was applied. Incident light had a Gaussian distribution with a central wavelength of 632.8 nm and a half width of 265 nm, and was polarized along the $x-$axis.

2. Interaction Between Nano-size Cylinders

In order to confirm the optical interaction between nano-sized metal materials, the optical properties of a small number of metal array structures were investigated. For this purpose, the light intensity distribution of a single material, a lateral single column array structure, and a multi-column array structure was comparatively analyzed.

Figure 1 shows the distribution of the pointing vector and electric field on the $x-z$ plane when light polarized in the $x-$direction is perpendicularly incident on the interface. The simulation space is 0.5 μm × 0.5 μm × 0.5 μm, and the diameter and length of the cylinder are 20 nm and 500 nm, respectively. In Figure 1 (a) ∼ (c) is the result of cylinder array for 1 × 1, (d) ∼ (f) is 5 × 1, and (g) ∼ (i) is 5 × 5. The real component of the electric field appears relatively clearly in the $x-$direction, but rapidly weakens in the $z-$direction of (h). This is because the incident light is polarized in the $x-$direction. On the other hand, the imaginary component of the electric field shows a clear distribution in the entire area in all cases.

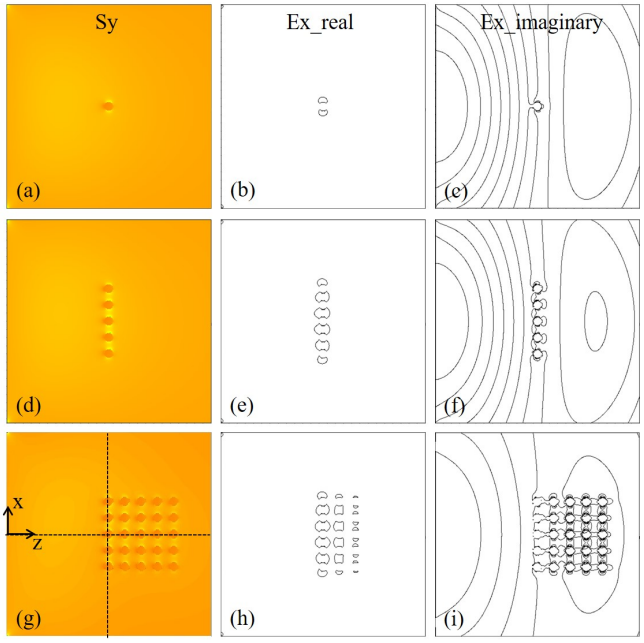

Figure 1. *$x-z$ plane pointing vector and electric field component for 1 × 1, 5 × 1, and 5 × 5 nano-size cylinder*

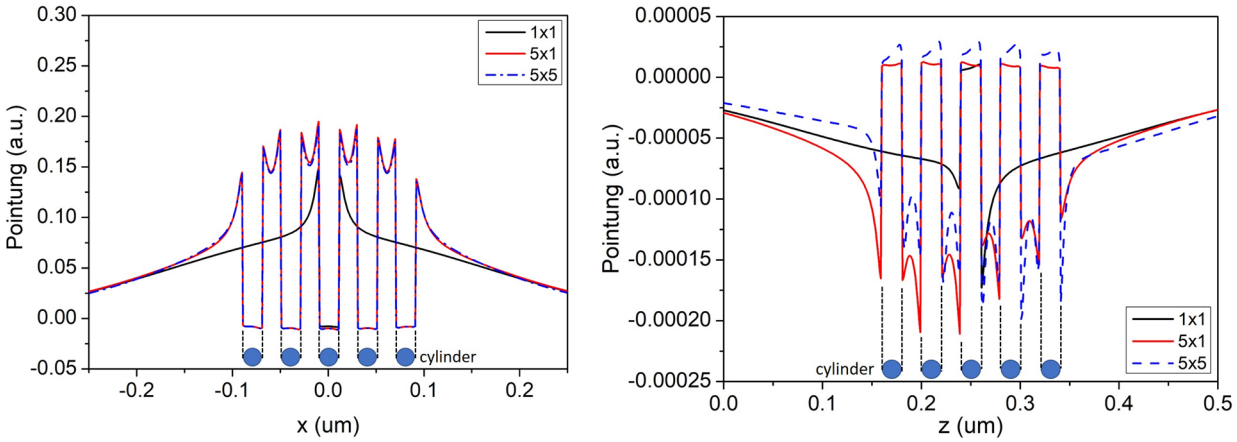

Figure 2. *Pointing vector distribution versus transverse (a) and longitudinal direction (b).*

Figure 2 shows the distribution of real components of the pointing vector, Sy, measured in the lateral direction ($x-$direction) and longitudinal direction ($z-$direction) in the $x-z$ plane (Figure 1). The strength of the pointing vector at the cylinder position is almost zero. In the space between the cylinders, there is a curvature, and it is the peak value on the left and right surfaces of the cylinder. Figure 2(a) shows a lateral distribution, and since the incident light is polarized in the $+x$ direction, the peak value in the $+x$ direction is slightly high. There is no difference in the magnitude of the peak value in the 5×1 and 5×5 structures.

Figure 2(b) shows a vertical distribution, and peaks occur on the front and rear surfaces of the cylinder. The peak values are different in the 5×1 and 5×5 structures. This is different from the characteristic in the lateral distribution. This clearly seems to be because the interaction pattern in the array structure is different. That is, in the metal plate, only the lateral interaction contributes to the spatial field distribution. However, in the case of [10, 11, 12], cylinder, multiple interactions not only in the lateral and longitudinal directions but also in the oblique direction contribute to the field distribution. In the 5×1 structure, only lateral interactions occur as in the plate structure, but in the 5×5 structure, multiple interactions occur.

3. Layer Effect

In this section, we intend to analyze the optical properties of the structure in which nano-size cylinders are distributed in a wider space. The simulation analysis area and cell size directly affect the computation time. If the analysis area is large, the computation time of the computer increases proportionally. On the other hand, as the cell size increases, the calculation time decreases. However, if the cell size is set to be larger than the appropriate size, the nano effect may be omitted from the calculation result. Therefore, it is very important in nano-optical research to determine the analysis area and cell size at an appropriate level.

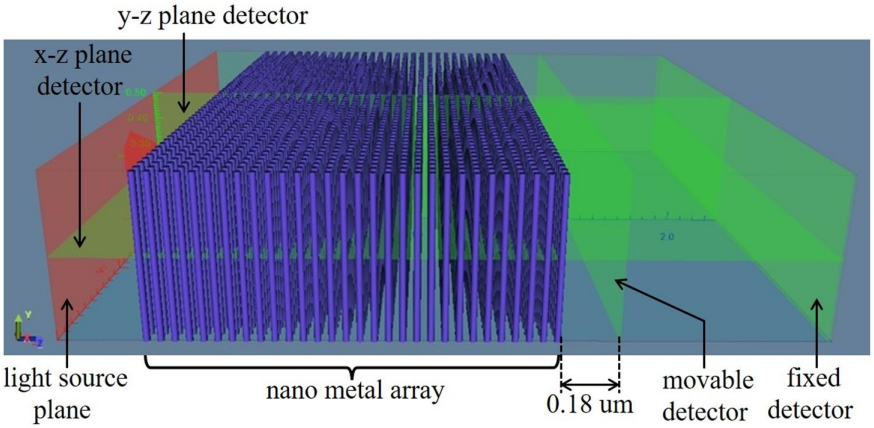

Figure 3. *Nano-size cylinder layer effect simulation model.*

In this study, in order to analyze the optical effect of an array of nano-sized metal materials, we set the simulation space to 2.0 μm $\times$ 0.5 μm $\times$ 2.2μm was set as shown in Figure 3. In addition, the FDTD simulation cell size was set to 4 nm so that the nano-effect was not omitted. In a previous study, it was investigated that a cell size of 5 nm gave sufficiently accurate results[11]. We set the boundary conditions so that all electric and magnetic fields reaching the simulation boundary are absorbed. This is to prevent the field reaching the interface from being reflected back and affecting the optical properties. Incident light is emitted at $z = 0$ and travels in the $+z$ direction, and the first column of the metal array starts at 0.25 μm.

In the case of subwavelength-thick metal plate array structures, a strong and continuous lateral interaction occurs between adjacent plates while light passes through them. Therefore, focusing and negative refraction phenomena clearly occur. [11] On the other hand, in the case of a periodic metal array with a subwavelength diameter in the shape of a cylinder and a sphere, the lateral interaction is weakened and multi-interaction occurs. This is because there is no continuity of material in the longitudinal direction in structure. Accordingly, focusing and negative refraction are somewhat weakened, and diffraction occurs due to the grating structure. As a result, beam splitting occurs depending on the condition of the incident light.

Figure 4 shows the light transmittance for the metal cylinder array. The light intensity was measured by two detectors installed on the $x - y$ plane in Figure 3. One is a movable detector installed at a certain distance (0.18 μm) from the end of the metal array, and the other is a detector installed at a fixed location ($z = 2.19$ μm).

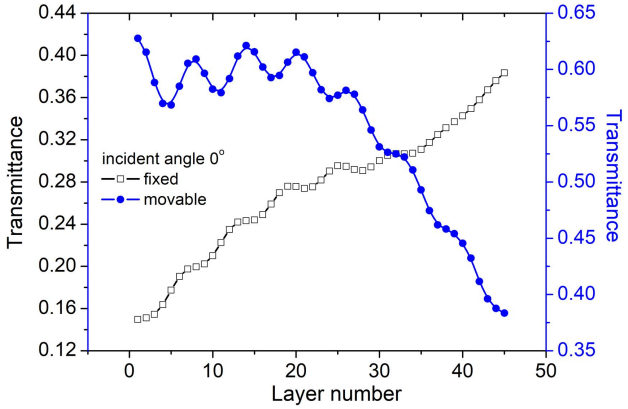

Figure 4. *Light transmittance for light normal incident.*

The blue solid circle in Figure 4 is the result measured by the movable detector. As the number of layers increases, the transmittance decreases. This is due to the attenuation by the spread of light and absorption by the metal as the light propagates through the medium space. A distinctive feature is the periodicity of transmittance as the number of layers increases. Transmittance periodicity was shown throughout the graph. Moreover, it oscillated up to about 20 layers, but the transmittance did not decrease. After the 20th layer, although the oscillation of transmittance appeared weakly, it decreased sharply. This result is considered to be because the beam propagation tendency is strong in the front part of the metal array, but the beam spread is strengthened as the scattering effect by each cylinder becomes stronger toward the back.

The intensity of the result (open rectangle) measured by the fixed detector increases as the number of layers increases.

The direct reason is that as the number of layers increases, the distance between the fixed detector and the end of the metal array becomes closer. When light propagates through an empty space, the intensity decreases as it diverges. Although the intensity is weak even when light passes through the space of the metal array, the degree of decrease is relatively small compared to the degree of attenuation in the empty space. This seems to be due to the redistribution of light intensity in space by the interaction between metal materials. This phenomenon shows the possibility of using nanomaterials as energy transfer[16].

Figure 5(a) is the magnetic field, Hy distribution in the $x-z$ plane ($y = 0$) for the 45-layer array of cylinder metal. The intensity change appears periodically in the direction of travel, and the spread is weakened rather than proceeding through the empty space. Figure 5(b) is the electric field, Ex distribution in the $x - y$ plane (fixed detector $z = 2.19$ μm). In the case of a monolayer, the $x-$ and $y-$axis are symmetric similar to the characteristics of incident light. However, if the number of layers increases, the symmetry is broken by the influence of the polarization of the incident light ($x-$axis direction). However, beam splitting due to multiple gratings is not observed.

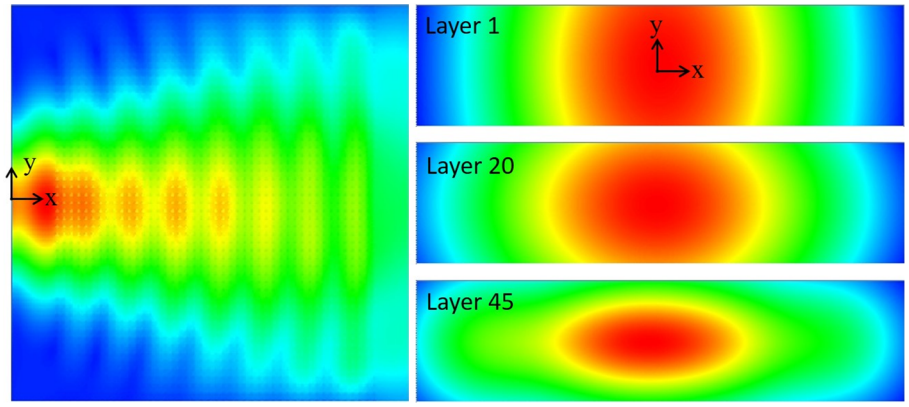

Figure 5. *Field distribution (a) Hy at $x - z$ plane (y=0) for 45 layers (b) Ex at $x - y$ plane (z=2.19 μm) for layer of 1, 20, and 45.*

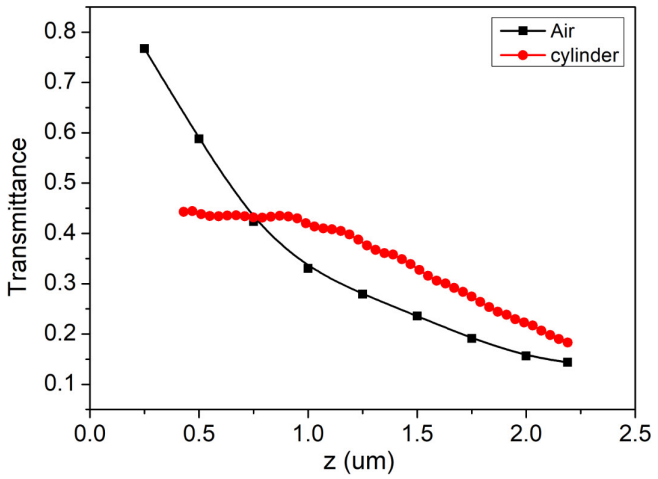

Figure 6. *Transmittance for air and metal cylinder array.*

Figure 6 shows the transmittance of light propagating through an air (solid-rectangle) space and a metal cylinder array (solid-circle) medium. The intensity of light propagating through empty space is rapidly weakened due to the spread. The intensity of light passing through the metal cylinder array is also weakened due to diffusion and absorption of the metal. However, as the number of layers of the metal cylinder increases, the subwavelength-sized metal fills the empty space, and as the light intensity is redistributed by the interaction between the metals, the diffusion becomes weaker. As a result, the light transmittance is increased when the metal is filled rather than when passing through an empty space.

4. Tilted Effect of Incidden Beam

In the previous section, the characteristics of transmitted light were analyzed when light was incident perpendicularly to the interface. In this section, the characteristics of transmitted light were analyzed when incident light was incident on the interface in an oblique direction (45°).

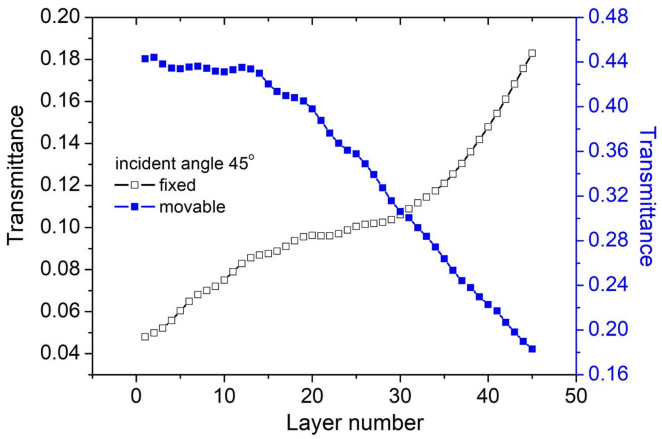

Figure 7. *Light transmittance for 45° incident.*

Figure 7 shows the light transmittance measured by the movable detector and the fixed detector. The overall trend

of oscillation and increase/decrease is similar to Figure 4, which is the case of normal incidence of light. The movable detector result is similar in that the oscillation phenomenon is weakened more rapidly (about 20 layers), but rapidly decreases thereafter. The result of the fixed detector shows a distribution with an inflection point of the increasing curve. On the other hand, the result of the fixed detector in Figure 4 is quite different from that showing an almost linearly increasing distribution except for the initial oscillation.

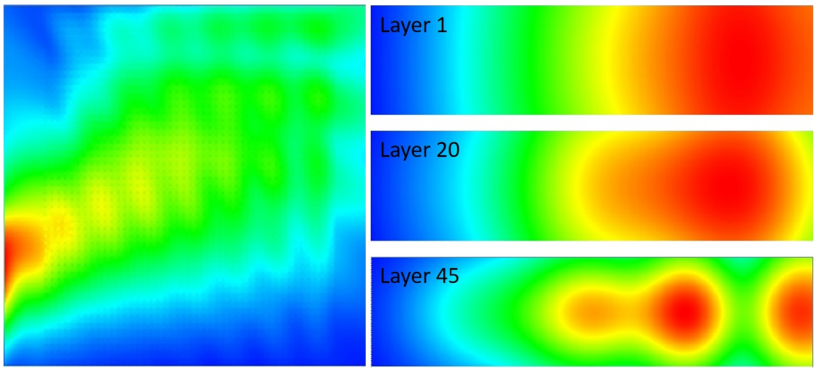

Figure 8. *Field distribution (a) Hy at $x-z$ plane (y=0) for 45 layers (b) Ex at $x-y$ plane ($z=2.19$) for layer 1, 20, and 45.*

Figure 8 (a) and (b) are the magnetic (Hy) and electric (Ex) field distributions, respectively. A marked difference from Figure 5, which is the result when the incident light is incident perpendicular to the interface, is observed. The splitting of the beam in the x-direction can be seen in Figure 8(a), which is the result in the $x-z$ plane. Figure 8(b) is the result in the $x-y$ plane according to the number of layers of the metal array. Here, too, as the number of layers increases, light splitting can be observed. As the number of metal layers increases, the beam splits in two. If the number of layers is further increased, the beam is divided into three branches. And the peak position of the intensity distribution moves in the $-x$ direction. The reason that the beam splitting phenomenon cannot be explained simply by diffraction is that the beam splitting does not appear when light is vertically incident.

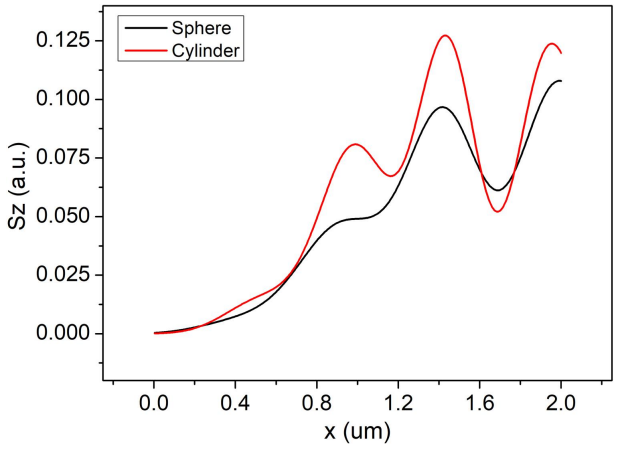

Figure 9. *Light intensity distribution of at $x-y$ plane($z=2.19\mu m$) for cylinder and sphere for 45 layers.*

Figure 9 is the distribution of the pointing vector in the $x-$direction in the $x-y$ plane ($z=2.19$ μm) for the 45th layer. Moreover, not only the cylinder metal array analyzed previously, but also the sphere (both diameter and spacing 20 nm) metal array results are shown. Cylinders are arranged in $y-$direction, so it is an array structure in $x-$ and $z-$directions. However, a sphere is a 3D array structure of $x-, y-$, and $z-$directions. Therefore, there are similarities between the two structures in the $x-$ and $z-$direction directions, but the structures are different in the $y-$direction direction. Accordingly, the similarity of the two structures is shown in the $x-$direction intensity distribution in Figure 9. In both structures, three peaks appear in the intensity distribution of the 45-layer metal array.

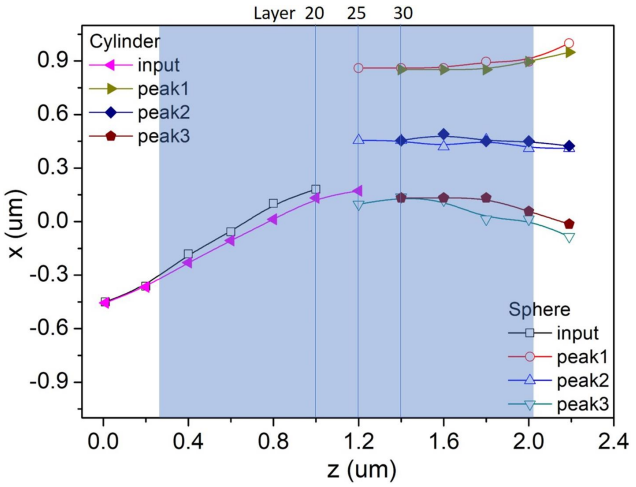

Figure 10. *Light intensity peak position.*

Figure 10 shows the intensity peak positions of light passing through a metal cylinder and a sphere array. The shaded area in the graph represents the 45-layer metal array section. Light is incident on the metal array area at 45° to the $+x$ direction from the starting point ($z=0.0$ μm, $x=-0.5\mu$m). In the case of cylinder, the beam proceeds in one line up to the 25th floor, and then splits into three lines. Between them, the beam splits

into two and ultimately into three. In the case of the sphere, it splits after the 20th layer. These results are respectively related to the solid-circle distribution in Figure 7. In the case of cylinder, the transmittance oscillates, and it decreases rapidly after passing the 25th layer. Therefore, it seems that the sharp decrease in the intensity of the transmittance in Figure 7 causes the intensity to decrease in the propagation direction as the beam splits and spreads in the array structure.

5. Summary

In this study, the optical properties of subwavelength-sized metal array structures were analyzed. For this purpose, light distribution and light transmittance in the cylinder array structure were investigated. Multiple interactions between metal materials occurring in the array structure affect the spatial field distribution. This caused a difference in the distribution of the longitudinal pointing vector in the 5×1 structure and the 5×5 structure. The light transmittance was higher when passing through the nano-size metal layer than through the empty space. This is a result that cannot be explained simply by diffraction in a regular array structure. In addition, when the number of array layers increased when light was incident on the interface in an oblique direction, the beam was split into several strands. This phenomenon occurred after about 20 layers, and showed almost similar results in the cylinder array and sphere array structures. Combining the results of this study, it is expected that various applications such as energy transfer can be confirmed through a more detailed analysis of multiple interactions occurring in the subwavelength size metal array structure.

References

[1] T. W. Ebbesen, H. J. Lezec, H. F. Ghaemi, T. Thio, P. A. Wolff (1998) Extraordinary optical transmission through sub-wavelength hole arrays, Nature 391, 667-669. doi: 10.1038/35570.

[2] W. L. Barnes, A. Dereux, T. W. Ebbessen (2003) Surface plasmon subwavelength optics, Nature 424, 824-830. doi: 10.1038/nature01937.

[3] Q.-H. Park, K. G. Lee and D. S. Kim (2006) Influence of surface plasmon polaritons on light transmission through metallic nanoslits, J. Korean Phys. Soc. 49, 2075-2079.

[4] H. A. Bethe (1944) Theory of Diffraction by Small Holes, Phys. Rev. 66, 163-182. https://doi.org/10.1103/PhysRev.66.163

[5] T. Thio, H. J. Lezec, T. W. Ebbesen, K. M. Pellerin, G. D. Lewen, A. Nahata, R. A. Linke (2002) Giant optical transmission of subwavelength aperture: physics and applications, Nanotechnology 13, 429-432. doi: 10.1088/0957-4484/13/3/337.

[6] F. J. Garcia, H. J. Lezec, T. W. Ebbessen, L. Martin-Moreno (2003) Multiple paths to enhance optical transmission through a single subwavelength slit, Phys. Rev. Lett. 90, 213901. doi: 10.1103/PhysRevLett.90.213901.

[7] L. Martin-Moreno, F. J. Garcia-Vidal, H. J. Lezec, A. Degiron, T. W. Ebbessen (2003) Theory of highly directional emission from a single subwavelength aperture surrounded by surface corrugations, Phys. Rev. Lett. 90, 167401. https://doi.org/10.1103/PhysRevLett.90.167401

[8] H. J. Lezec, A. Degiron, E. Devaux, R. A. Linke, L. Martin-Moreno, F. J. Garcia-Vidal, T. W. Ebbessen (2002) Beaming light from a subwavelength aperture, Science 297, 820-822. doi: 10.1126/science.1071895.

[9] Y. C. Kim, D. W. Kim, V. K. Jha, O. K. Suwal, S. S. Choi (2011) The effect of groove on the light transmission through nano-apertures, Physica E: Low-dimensional Systems and Nanostructures, 43, 929-933. doi: 10.1016/j.physe.2010.11.019.

[10] HERMANN A. HAUS, AND LYNNE MOLTER-ORR (1983) Coupled Multiple Waveguide Systems, IEEE JOURNAL OF QUANTUM ELECTRONICS, VOL. QE-19, 840-844. doi: 10.1109/JQE.1983.1071950.

[11] Xiebin Fan and Buo Ping Wang (2006) Nanoscale metal waveguide arrays as plasmon lenses, Optics Letters 31, 1322-1324. https://doi.org/10.1364/OL.31.001322

[12] T. Pertsch, T. Zentgraf, U. Peschel, A. Br$\tilde{A}$uer, and F. Lederer (2002) Anomalous Refraction and Diffraction in Discrete Optical Systems, PHYSICAL REVIEW LETTERS 88, 093901. https://doi.org/10.1103/PhysRevLett.88.093901

[13] Shunsuke Murai, Takuya Tsujiguchi, Koji Fujita, and Katsuhisa Tanaka (2011) Enhanced form birefringence of metal nanoparticles with anisotropic shell mediated by localized surface plasmon resonance, OPTICS EXPRESS 19, 23581-23589. https://doi.org/10.1364/OE.19.023581

[14] A. J. Waddie, R. Buczynski, F. Hudelist, J. Nowosielski, D. Pysz,2 R. Stepien, and M. R. Taghizadeh (2011) Form birefringence in nanostructured micro-optical devices, OPTICAL MATERIALS EXPRESS 1, 1251-1261. https://doi.org/10.1364/OME.1.001251

[15] Jiha Sung, Maxim Sukharev, Erin M. Hicks, Richard P. Van Duyne, Tamar Seideman, and Kenneth G. Spears (2008) Nanoparticle Spectroscopy: Birefringence in Two-Dimensional Arrays of L-Shaped Silver Nanoparticles, J. Phys. Chem. C 112, 3252-3260. doi: 10.1021/jp077389y.

[16] P. Andrew and W. L. Barnes (2004) Energy Transfer Across a Metal Film Mediated by Surface Plasmon Polaritons, SCIENCE 306, 1002-1005. doi: 10.1126/science.1102992.